Zeitschrift: Helvetica Physica Acta
Band: 47 (1974)
Heft: 5

Artikel: Abrasion: a new powerful technique for ultraclean investigation of the gas/solid interface : application in the case H2/Ni

Autor: Antonini, F.

DOI: https://doi.org/10.5169/seals-114581

Helvetica Physica Acta
Vol. 47, 1974.
Birkhäuser Verlag Basel

Abrasion: A New Powerful Technique For Ultraclean Investigation of the Gas/Solid Interface

Application in the Case H_2/Ni

by **J. F. Antonini**
Battelle Geneva Research Centre

(16. V. 74)

Abstract. Application of the abrasion technique – see preceding paper – for H_2/fresh nickel surfaces interaction illustrates how reliable the results are, when counter-flux during adsorption/desorption measurements is not neglected and numerous measurements are involved.

In the range [–20°, 100°C], H_2 adsorbs without activation into three atomic states: a mobile precursor P, a chemisorbed C, a high temperature, probably 'bulk phase', S.

The heat of adsorption in the C state is 14.5 ± 0.5 kcal/mole, independent of the population of this state. The desorption reaction from C and P is a second-order reaction with activation energy 14 kcal/mole from C. These results are in good agreement with the literature, despite the unfamiliar nature of fresh surfaces.

1. Introduction

The system H_2/Ni is and has been the subject of numerous studies, starting early in the century up to the most recent publications, involving most of the possible combinations between the different shapes for the Ni sample (film, ribbon, wire, single crystal, powder, supported small crystals, etc.) and the techniques available. Although some results are still controversial, as the dependence of the activation energy for desorption with the surface population σ, H_2/Ni constitutes a good choice for checking the feasibility of a new technique experimentally, namely the technique of abrasion [1].

2. General Description of the Equipment

2.1. UHV chamber

The UHV chamber is a 4.5 litre stainless-steel vessel, to which the following fixtures are attached:

— a miniature B-A total pressure gauge, used only during bake-out and UHV conditioning of the chamber, otherwise always isolated from the UHV chamber by a glass valve so as to prevent all stray interactions of the BAG with the gas phase;
— an Omegatron-type MS fitted with a low-temperature oxide-coated cathode, in order to minimize the unavoidable interactions with the gas phase;

— a leak valve for introducing the reagent grade gas (99.99% spectroscopically pure H_2);
— the experimental cell (see 2.3) containing the nickel sample to be abraded, the heating facility, the thermocouples, etc.;
— the mechanical device for abrasion;
— the pumping valve.

2.2 Pumping system

The pumping system is conventional, comprising a mechanical pump, a three-stage oil (DC 704) diffusion pump (S = 6 l/s for N_2), and an activated zeolite trap. The ultimate pressure attainable after bake-out is limited to 4.5×10^{-9} Torr H_2 by hydrogen diffusion out of the stainless-steel walls. Apart from H_2, the only measurable gas contribution in the mass spectrum is a 5×10^{-11} Torr (N_2 equiv.) peak at M28, probably CO produced by the MS cathode itself.

2.3. Experimental cell (see Fig. 1)

Located opposite the mechanical device for abrasion (see 2.5), the experimental cell is designed in such a way as to allow abrasion of the ultra-pure Ni sample at constant adjustable temperature and thermal desorption (mainly at constant temperature by a step heating programme) of the adsorbed gas to be conducted in the cleanest conditions.

It is of cylindrical symmetry and consists mainly of an ultra-pure nickel tube (3) and another nickel tube (4) of the same dimensions, welded together along (6) but separated by a tight wall (5) and both surrounded by a quartz fabric and a heating filament coil (11).

The section including the ultra-pure nickel opens into the UHV chamber for adsorption and desorption measurements; the other section is intended to measure and regulate the temperature by means of two separate thermocouple circuits (9). A thermal barrier (2) with water circulation ensures a stable temperature of the UHV

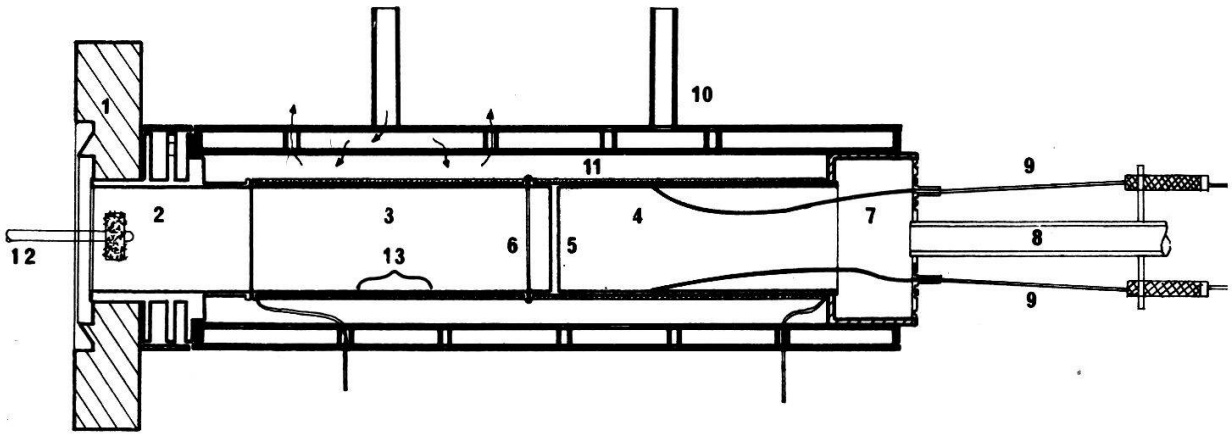

Figure 1
Experimental cell. 1) Conflat flange; 2) thermal barrier with water circulation; 3) ultrapure nickel tube sample; 4) twin nickel tube for thermal regulation; 5) tight wall; 6) annular welding between tubes 3) and 4); 7) flange for thermocouples feedthrough; 8) brazed copper tube for pinch-off; 9) thermocouples (Thermocoax Philips); 10) air cooling system; 11) heating filament coil; 12) abrading tool; 13) location of the abraded area.

chamber whatever the temperature of the experimental cell. Both sections are surrounded by a common air-cooling system for long-term stability or fast step-increase of the temperature of the nickel tube. Both sections have been proved to be thermally identical, and the temperature of the zone of ultra-pure nickel sample (3) intended to be abraded (13) has been checked to be homogeneous, and the indications of both thermocouples agree within 1° between 77°K and 450°K.

2.4. *Ultra-pure nickel tube (3)*

This part of the experimental cell is made of a 4.8 N nickel sheet supplied by Koch-Light[1]). Once laminated, coiled into a cylinder, welded, electropolished and rinsed, but before incorporation into the experimental cell, the nickel sample was submitted to a 36-day programme of cleaning by successive oxidation-reduction cycles. The total amounts of carbon and sulphur which were given off mainly as CO, CO_2, SO_2 (CH_4, C_2H_6, H_2S negligible) during the operation are estimated to be 2.5×10^{18} C atoms and 4×10^{17} S atoms, corresponding respectively to 10 p.p.m. and 2 p.p.m. or to 30 monolayers! This time-consuming procedure has to be considered here as a *bulk* purification together with an illustration of the credibility in the claims for purity by the suppliers. It was stopped before exhaustion of the impurities, since exhaustion is not required by the abrasion technique.

2.5. *Mechanical device for abrasion (see Fig. 2)*

The device used for this study is derived from a primitive design developed for a research programme on glass [2–4]. It consists of a diamond (or alumina) tool (2)

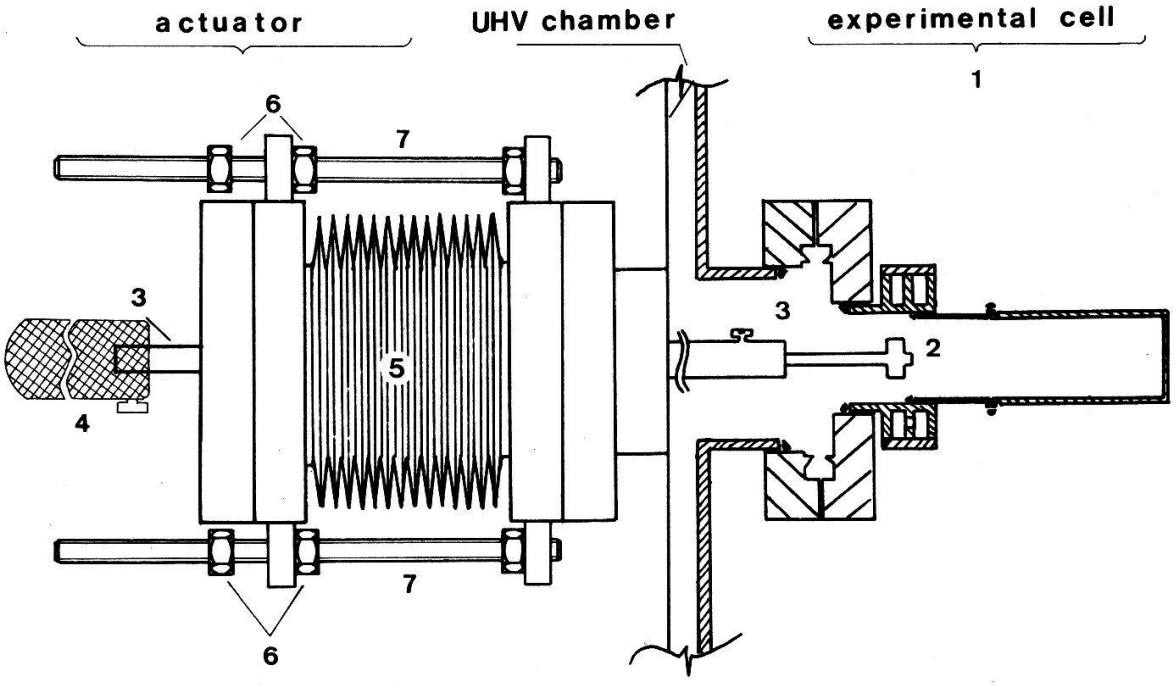

Figure 2
Mechanical device for abrasion. 1) Experimental cell (see detailed sketch, Fig. 1); 2) abrading tool; 3) holder of abrading tool; 4) handle; 5) metallic bellows; 6) adjustable nuts; 7) guide-screws.

[1]) The analysis of impurity content given by the supplier is the following (in p.p.m.): Ag < 1; Al: 1; Ca < 1; Cu < 1; Fe: 3; Mg: 1; Si: 2; no carbon.

actuated manually from outside the UHV chamber via metallic bellows (5). The tool can be introduced into the experimental cell (1), pressed against the inner surface of the nickel tube, moved back and forth as many times as desired (usually only once so as to take advantage of the shortest transient time). Two pairs of adjustable nuts (6) on two guide-screws (7) serve to locate the abraded zone of the nickel tube and maintain a constant stroke. Apart from this, there is no provision for other parameters to be controlled.

The amplitude of the temperature rise which may occur just below the cutting tool was calculated in the case of diamond on Ni and found to be limited to 50°C and to decay below 1°C within one second.

3. Experimental Procedure

Once absolute calibration of the MS and of the pumping speed is established, the standard procedure outlined in the preceding paper is followed. H_2 is introduced via the leak valve and a dynamic equilibrium pressure p_{01} is established. The abrading tool is pressed against the nickel tube and moved once back and forth[2]) between the limits fixed by the nuts (in this case a course of 8 mm in 0.6 s). The adsorption curve $p_{01} - p(t)$ is recorded under these conditions of T and p_0. After modification of the H_2 flux in order to establish another equilibrium pressure p_{02}, a similar abrasion is repeated and the new adsorption curve $p_{02} - p(t)$ recorded. A set of ten to fifteen different values of p_{0i} scanned for a given constant temperature and a set of nine different temperatures (–20°; 0°; 20°; 30°; 40°; 50°; 60°; 80°; 100°C) are estimated to be sufficient to provide a detailed description of the interaction of H_2/Ni.

The adsorption curves are recorded by a digital voltmeter with a printer at a sampling rate of usually 1 or 2 per s and simultaneously displayed by a stripchart recorder (see Fig. 3). The printed data of the digital voltmeter are used to compute

$$\sigma(t), \quad \frac{d\sigma}{dt} \quad \text{and} \quad \frac{p_0 - \tau\dfrac{dp}{dt} - p(t)^3)}{p(t)}.$$

No attempt has been made to use the computer further. In fact, the $\sigma(t)|_{p_{0i}}$ data are plotted on a large-scale millimetric chart and the rest of the calculation is made manually, namely the graphical determination of the slopes $d\sigma/dt|_{\sigma_j}$ as a function of p_{0i} for the different σ_j. Figure 4 shows the result for 40°C when $d\sigma/dt$ is plotted as a function of $f(p_0)$, according to the model designed for the interpretation of the adsorption measurements by abrasion (see preceding paper). The log–log plot allows the determination of the unknown function $f(p_0)$. Figure 5 shows the same type of data, but for another temperature (0°C), when plotted in lin–lin scale. The last figure illustrates the excellent agreement between the model predicting a linear dependence of $d\sigma/dt$ as a function of $f(p_0)$ and the experiment.

Such straight lines allow the determination of the adsorption term $k_A g(\sigma)$ by the slope and of the desorption flux $k_D h(\sigma)$ by the intercept with the origin.

Application of the model is in fact not restricted to isothermal adsorption but must extend to isothermal desorption experiments too.

---

[2]) The notation adopted for an abrasion by N back and forth movements is N × G_2.

[3]) This ratio is proportional to the overall sticking probability.

For isothermal desorption experiments, the procedure is the following: the inner surface of the Ni tube is first passivated by means of a slight oxidation. A fresh surface is then created once for all by multiple abrasions and exposed to a dynamic equilibrium

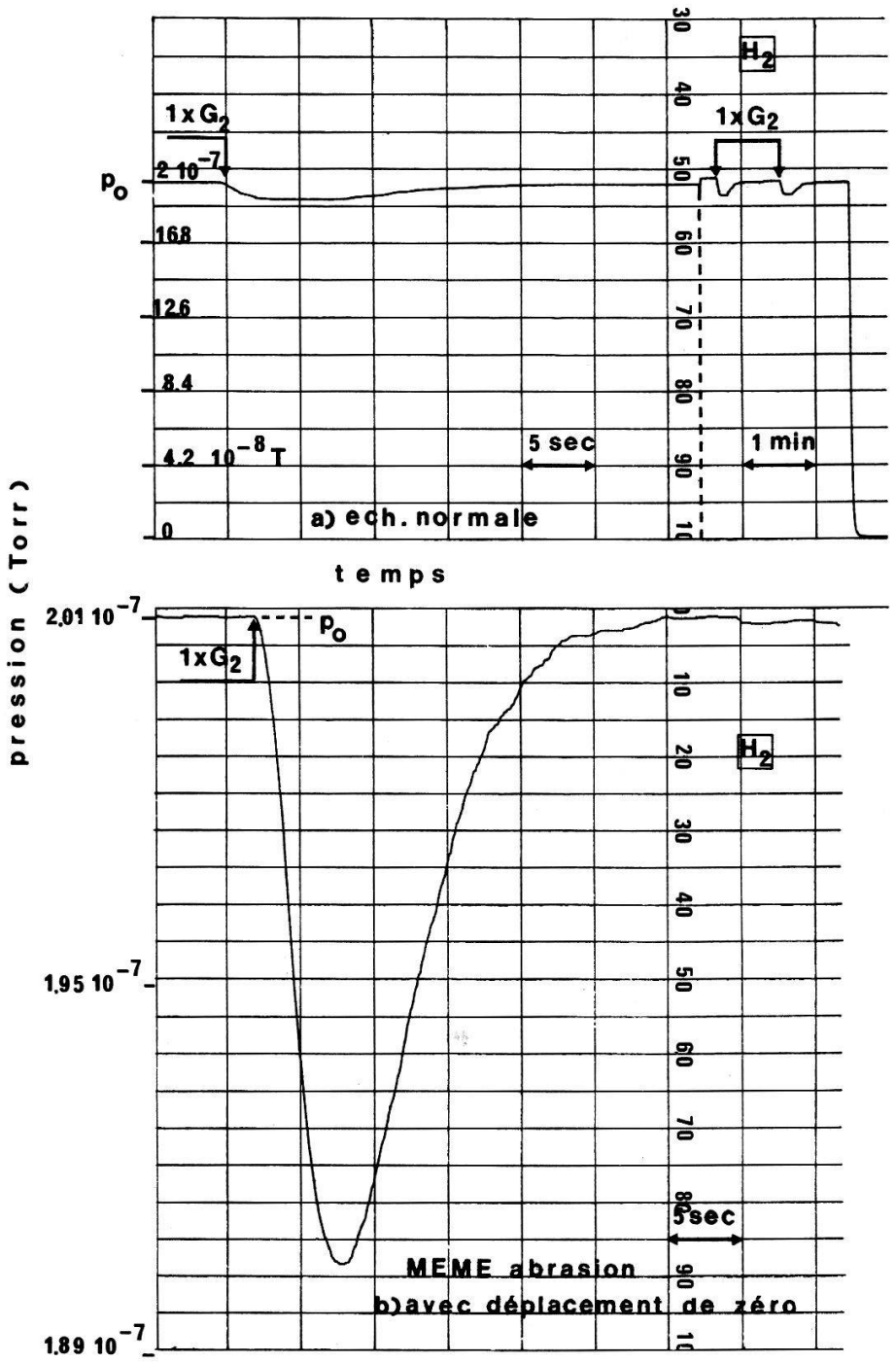

Figure 3
Typical H_2/Ni adsorption curves. *N.B.* The chart below represents the same adsorption curve as above, but with higher amplification of the electrometer and zero suppress function on.

pressure p_0. Once both T and p_0 are constant, the temperature is suddenly raised to a higher constant temperature and the desorption curve recorded. Different temperature steps are applied for a given value of p_0, say p_{0i}, and the procedure is repeated for different pressures p_{0j} $(j \neq i)$.

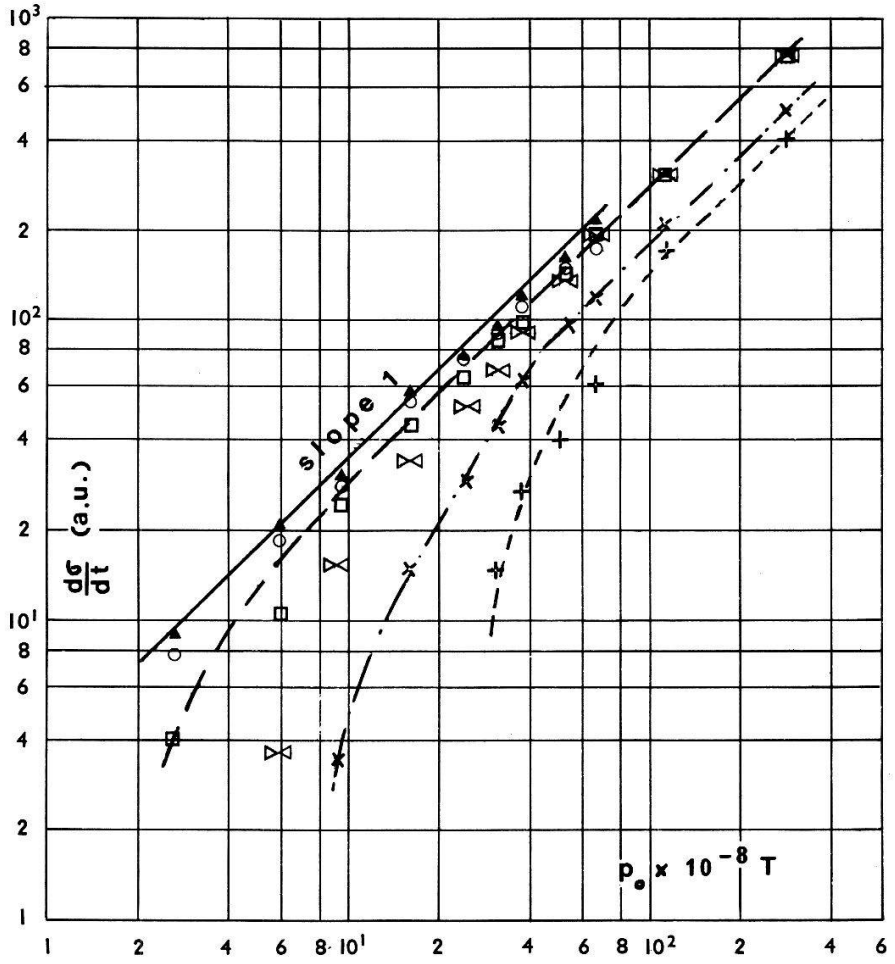

Figure 4
Overall adsorption flux as a function of $f(p_0)$ for $T = 40°C$ at different constant surface coverages θ (log–log plot). ▲: $\theta = 5\%$; ○: 10%; □: 15%; ⋈ : 20%; ×: 25%; +: 30%.

The experimental cell is designed in order to allow such thermal desorption by a step-heating programme.

Some results obtained under such conditions are reported in paragraph 6.3 and prove the self-consistency of the model, i.e. that the unknown functions p_0, k_A, k_D, $g(\sigma)$, $h(\sigma)$ could, theoretically, also be obtained by isothermal desorption data.

4. Correction Factors for Lowering Dispersion Between Successive Abrasions

A fresh surface by abrasion is characterized by its apparent area A' responsible for the exchange rates between gas phase and surface phase populations, and its true area A, responsible for equilibrium surface population at saturation (see Fig. 7). Since the model (1) is based on comparison between adsorption curves recorded under different experimental conditions of T and p_0, it is of prime importance that the abrasions yielding the adsorption curves are fully reproducible, i.e. with constant A' and A areas. As the actual mechanical device for abrasion was far from ideal, it was necessary to find a way of circumventing its poor reproducibility. Note that this is inherent not to the abrasion technique, but to the device used.

Variation of pressure $p(t)$ inside a vacuum system containing a surface sample, induced by the variation of surface population of the sample — for instance the expression of the adsorption curve in the case of abrasion – is given by solving the

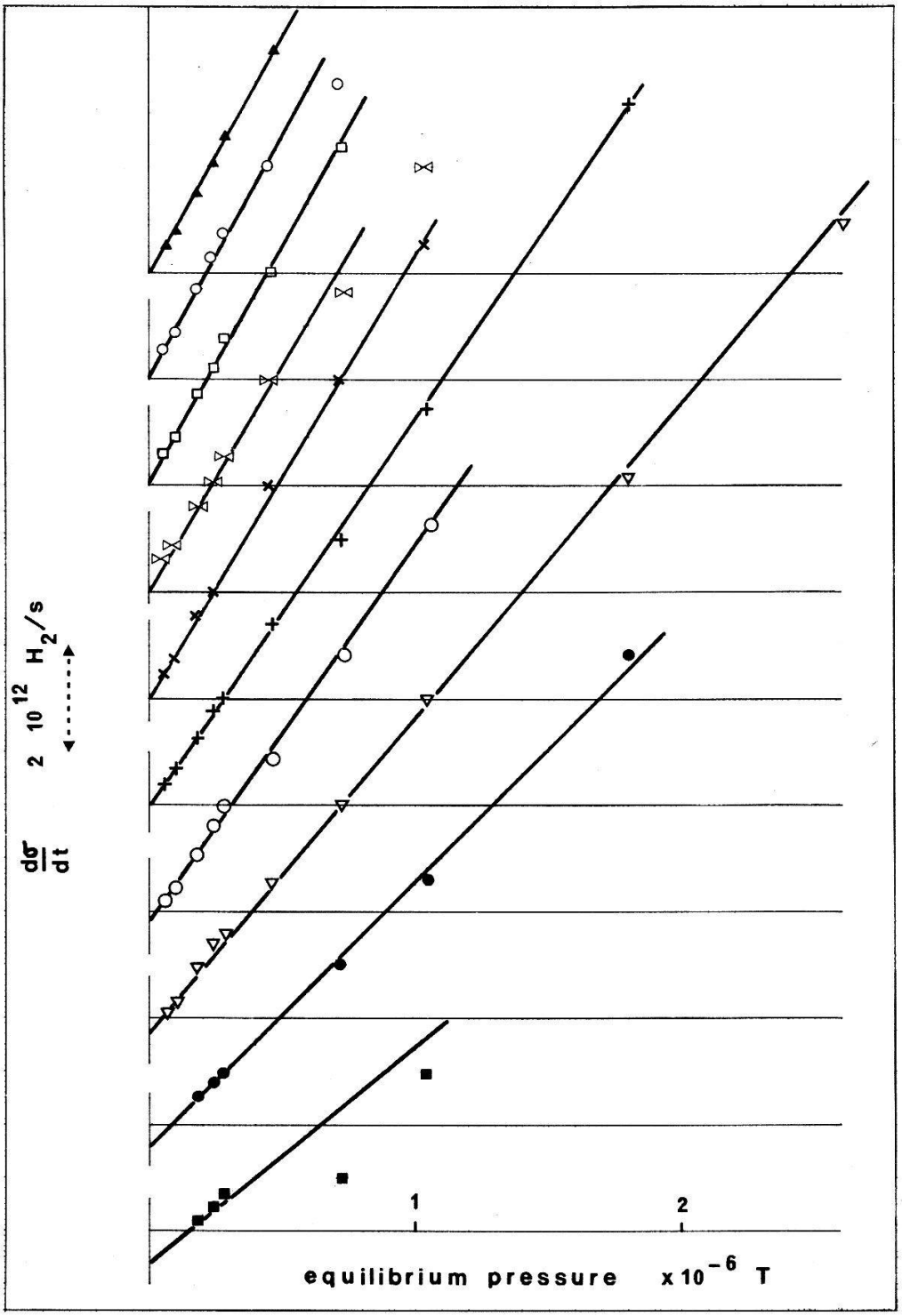

Figure 5
Overall adsorption flux as a function of p_0 for $T = 0°C$ at different constant surface coverages θ (lin–lin plot). △: $\theta = 5\%$; ○: 10%; □: 15%; ⋈: 20%; ×: 25%; +: 30%; ○: 45%; ▽: 50%; ●: 59%; ■: 65%.

following system of equations:

$$\begin{cases} KV\dfrac{dp}{dt} = -KSp + q_0 - A\dfrac{d\sigma}{dt} \\ A\dfrac{d\sigma}{dt} = A' k_A f(p_0)\, g(\sigma) - A' k_D h(\sigma). \end{cases}$$

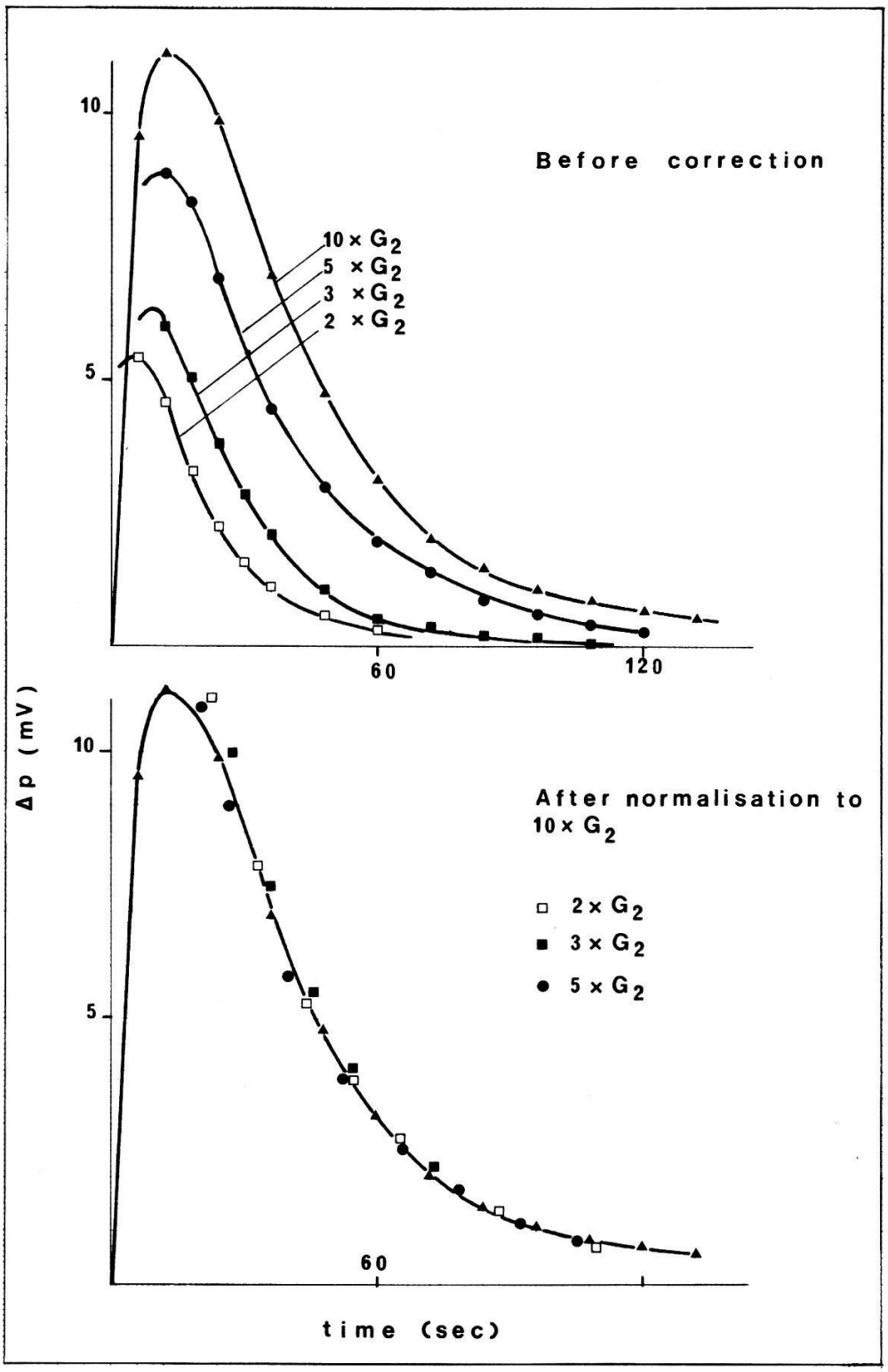

Figure 6
Determination of the efficiency of the normalization procedure applied on four different adsorption curves.

The general solution clearly cannot be found in a closed form when the surface population changes according to the adopted model, except under particular conditions. By chance, the conditions allowing the system to be integrated hold very well in our case and the resulting particular solution, made up of two exponential functions, shows that the magnitude of the pressure variation depends on A' and the saturation

time on the ratio A/A' [5]. These simple dependences allow the adsorption curves to be normalized so that they all look like being produced by similar abrasions with standard A' and A areas, supposed to be independent of T and p_0.

For each abrasion, the actual gas uptake, which is proportional to the true area A, is measured and compared with that predicted by the isotherm curves[4]). The comparison provides the factor by which the actual true area A departs from the standard value A_{standard} expected from a completely reproducible abrasion. The standard value A_{standard} is chosen so that most of the ratios A/A_{standard} are close to 1.

For each abrasion, the actual saturation time constant A/A' is measured and compared with a standard value $A/A'|_{\text{standard}}$. Comparison provides the first correction factor. The $A/A'|_{\text{standard}}$ is chosen so that most of the correction factors $(A/A')/(A/A')|_{\text{standard}}$ are close to 1.

From A/A_{standard} and $(A/A')/(A/A')|_{\text{standard}}$, the second correction factor A', for the pressure variation, can be calculated.

An illustration of the efficiency of such a correction is given in Figure 6 where four adsorption curves, resulting from four deliberately very different abrasions $2 \times G_2$, $3 \times G_2$, $5 \times G_2$ and $10 \times G_2$ are compared and normalized with respect to one of them (the $10 \times G_2$ curve). In the real case, the dispersion between the curves is much more limited, coincidence being achieved with an accuracy better than 3%. This means that any adsorption curve can be corrected so that it coincides with the ideal curve, which would be obtained immediately with an ideal device capable of fully reproducible abrasion, within less than 3%.

5. Experimental Results

5.1. Morphology of a freshly abraded Ni surface

Figure 7 illustrates the intersection of two furrows as obtained with a diamond tool and a $5 \times G_2$ abrasion as obtained with the alumina tool. Ductility and spreading of the edges of the ridges by superposition of numerous abrasions are evident and lead to a difficult estimation of both A' and A.

An average value of A' was estimated both from Stereoscan photographs and from oxygen sticking probability measurements at liquid N_2 temperature, for which the different data found in the literature agree fairly well on the common single value 1 [6–9]. The two different estimations are close together within 20% if the initial sticking probability of O_2 is assumed to be equally unity on abraded surfaces. The common value is 0.0066 cm^2 for $1 \times G_2$.

The true area A was estimated both from low-temperature adsorption measurements of O_2, H_2 and CO up to completion of the monolayer and by establishing correlations between the curves $s(\sigma)$ giving the sticking probability of O_2 as a function of surface coverage determined by Klopfer on a polycrystalline nickel ribbon [10], or by Horgan and King on a nickel film [7], and on abraded surfaces [11]. The agreement between the different values of A obtained by the two methods is surprisingly good and leads to $A = 0.023$ cm^2 for $1 \times G_2$ and 0.11–0.12 cm^2 for $5 \times G_2$.

---

[4]) These isotherm curves (see Fig. 8) result from *numerous* adsorption curves, allowing accurate approximation, here based on the best power function fit. Moreover the adsorption curves result from $5 \times G_2$ abrasions, which are more reproducible than the $1 \times G_2$ ones.

Figure 7
Stereoscan views of freshly abraded nickel surfaces. No. 9: with a diamond tool, magnification: 600; slant angle: 60°; No. 2: with an alumina tool, magnification: 2250; slant angle: 60°.

5.2. Isotherms

Since a family of isotherm curves, based on numerous $5 \times G_2$ abrasions, has been established in order to circumvent the poor reproducibility of the abrasion, it was worth comparing these results, obtained under equilibrium conditions, with those obtained from adsorption measurements.

The isotherms are shown in Figure 8 for seven different temperatures between 0°C and 100°C, for a range of coverage extending approximately from 10^{-2} up to one monolayer. The curves are evidently intrinsically smooth, the elbows being due to the approximation method applied (least squares fit by a power function for each decade of pressure).

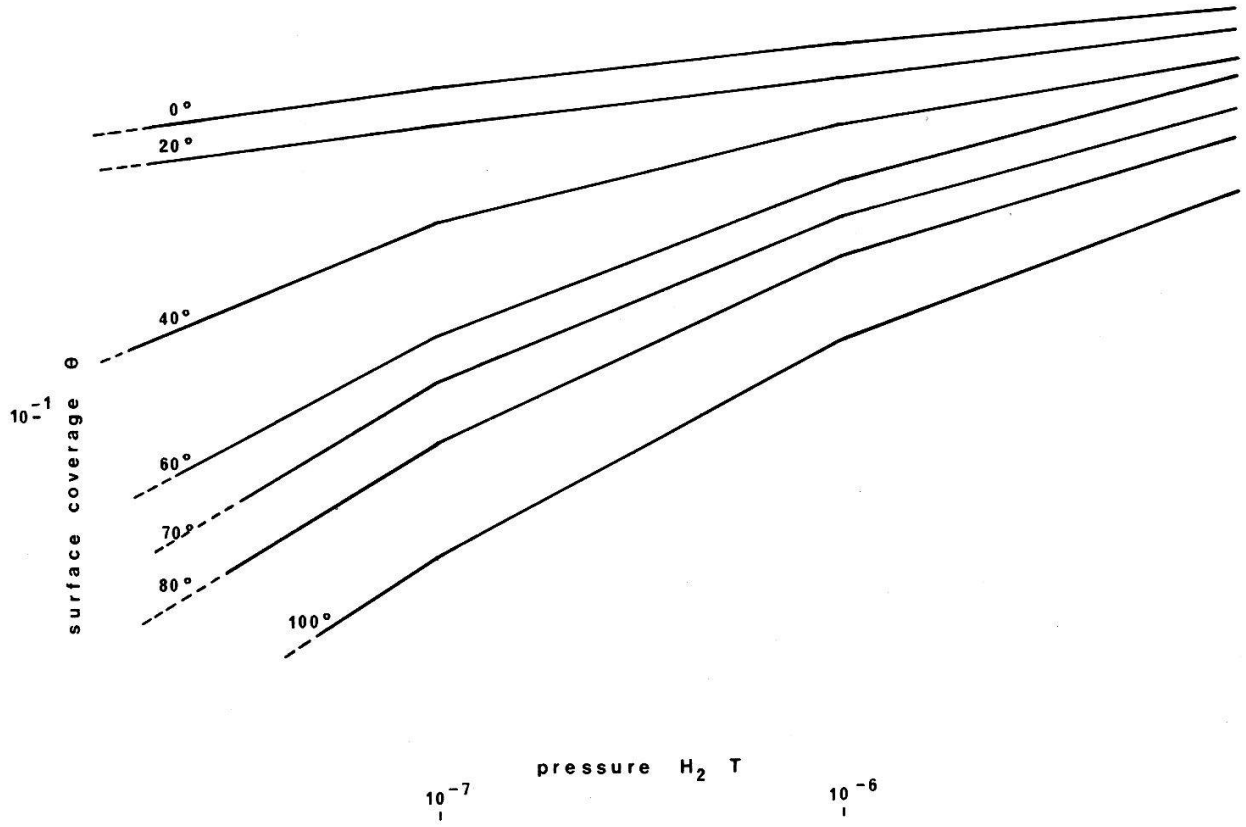

Figure 8
Isotherm curves for seven different temperatures between 0° and 100°C.

They provide quite linear isosters, from which the isosteric heat q_{iso} is drawn. q_{iso} is a constant in the investigated range of coverage θ ($4\% < \theta < 65\%$ of the monolayer defined as 2 H per surface Ni atom). The value is 14.5 ± 0.5 kcal/mole, quite comparable within the error domains with the activation energy E_D for desorption found from adsorption measurements (see Fig. 9). Since $q_{iso} = E_D$, the activation energy for H_2 adsorption on Ni has to be quite small, which is effectively found from adsorption measurements (see 5.6). The isosteric heat is consistent with the isobaric heat drawn from the isobars.

When plotted according to Freundlich's expression ($\sigma = cp^{1/n}$), the results are the following (see Table I).

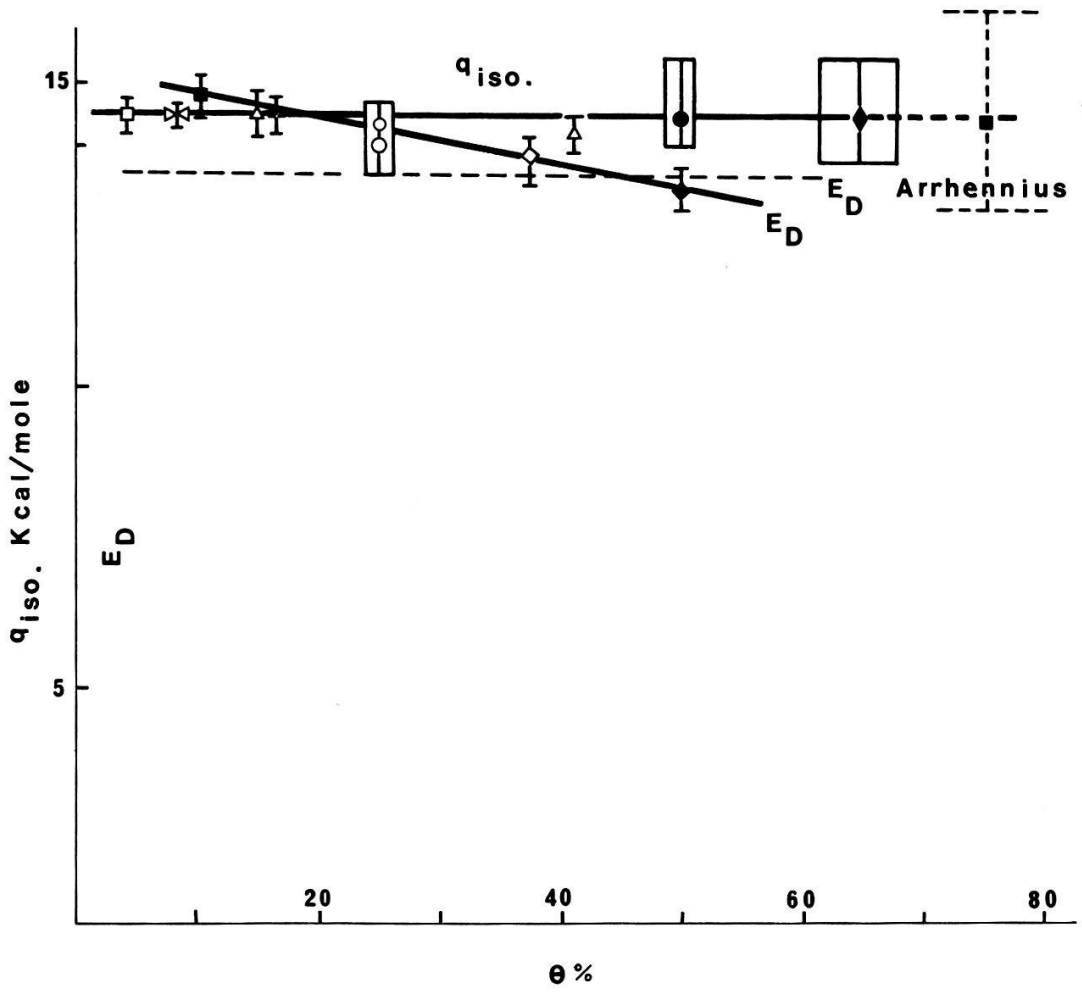

Figure 9
Dependence of the isosteric heat of adsorption q_{iso} and activation energy of desorption E_D as a function of surface coverage θ ($\theta = 100\%$ for 1 H_2/1 Ni).

If it is assumed that the reaction of H_2 desorption is second order ($h(\sigma) = \sigma^2$), which will be proved later (see 5.7), the equation of Freundlich's isotherm is, according to our model:

$$p_0 = \frac{k_D}{k_A} \frac{\sigma^2}{g(\sigma)}$$

or

$$\ln \sigma - \tfrac{1}{2} \ln g(\sigma) = \tfrac{1}{2} \ln p_0 - \tfrac{1}{2} \ln \frac{k_D}{k_A}$$

Table I

T (°C)	0	27	40	60	70	80	100
c	2.98	3.41	1.273	0.231	0.255	0.145	0.088
n	7.62	8	4.73	2.24	2.74	2.34	2.34
r	0.791_5	0.721_2	0.855_4	0.949_1	0.963_6	0.952_2	0.917_4

r = correlation factor.

which expresses a linear dependence between $(\ln\sigma - \frac{1}{2}\ln g(\sigma))$ and $\ln p_0$. When $g(\sigma)$ is a constant, the slope is $\frac{1}{2}$, decreasing as soon as $g(\sigma)$ starts to drop from 1 down to 0, according to the definition of $g(\sigma)$, without a necessary change in the adsorption heat. The behaviour of $g(\sigma)$, as obtained from adsorption measurements (see 5.5), is consistent with the isotherms.

5.3. *Definition of the monolayer*

In disagreement with all the data published in the literature, the surface population σ_{sat} at saturation on a freshly abraded Ni surface amounts to *2H atoms per 1 Ni surface atom* (surface density of Ni atoms: 1.7×10^{15} cm^{-2}). The maximum surface population which can cover the same abraded surface after a thermal desorption is limited to 1 H/1 Ni. This drop is not due to surface impurities, brought up by diffusion for instance, since successive desorption–readsorption cycles leave the usual ratio 1 H/1 Ni unchanged.

On a freshly abraded surface, there are really new adsorption sites which double the number of sites available on a normal clean surface. These supplementary and unsteady sites will be shown to be energetically indistinguishable from the steady sites.

It has to be noted that the absolute coverage appearing on the figures corresponds to 100% for a surface population σ of 2 H/1 Ni.

5.4. *Isosteric dependence of the adsorption flux on pressure*

This dependence is obtained by plotting $\ln d\sigma/dt$ as a function of $\ln f(p_0)$ (see Fig. 4). It is found that $f(p_0) = p_0$ for temperature lower than 60°C, which is a trivial result, generally postulated *a priori*. But for higher temperature, the asymptotic straight line for vanishingly small desorption flux definitively has a slope $\frac{1}{2}$, so that $f(p_0) = \sqrt{p_0}$, which is confirmed by the accurate alignment of $d\sigma/dt$ plotted as a function of $\sqrt{p_0}$.

An adsorption rate depending on $\sqrt{p_0}$ could be correlated with a diffusion process, especially for high temperature, where both solubility and diffusion rate for H_2/Ni could not be negligible. Such a dependence was already observed for H_2/Ni, H_2/Fe, O_2/W, Mo, Rh, N_2/Ta, Cr, Fe [12–14], generally together with an adsorption kinetics following the Elovich rate at room temperature and was shown [15] to be a surface reaction for H_2/Ni.

A possible explanation consists in postulating the existence of an *equilibrium of dissociation* in the overall adsorption reaction according to the following schemes:

$$\text{gas phase} \underset{}{\overset{K_1}{\rightleftharpoons}} \begin{matrix}\text{physisorbed}\\ \text{molecular phase}\end{matrix} \overset{K_2}{\rightleftharpoons} \begin{matrix}\text{precursor}\\ \text{phase } P\end{matrix} \xrightarrow{k} \begin{matrix}\text{chemisorbed}\\ \text{phase } C\end{matrix}$$

or:

$$\text{gas phase} \rightleftharpoons \begin{matrix}\text{precursor}\\ \text{phase } P\end{matrix} \rightleftharpoons \begin{matrix}\text{chemisorbed}\\ \text{phase } C\end{matrix} \xrightarrow{k} \text{new phase } S$$

The first hypothesis involves an equilibrium of dissociation between an atomic precursor state P for the atomic chemisorbed state proper C and the gas phase. Under such conditions and neglecting desorption from phase C:

$$[H_2] = K_1 p_0$$

$$[H^p]^2 = K_2[H_2]$$

$$\frac{d[H^c]}{dt} = k[H^p]$$

whence:

$$\frac{d[H^c]}{dt} = k\sqrt{K_2[H_2]} = k\sqrt{K_2 K_1 p_0} = k'\sqrt{p_0}$$

The second hypothesis involves the existence of a new activated surface or bulk phase (S) and again an equilibrium of dissociation, but this time between the chemisorbed phase C and the gas phase.

Distinction between the two hypotheses based only on the isosteric dependence of the adsorption flux on pressure is impossible; but the existence of a new phase S seems most probable, in view of the other results for $g(\sigma)$ and $h(\sigma)$ at high temperature (see Figs. 10 and 12).

5.5 Isothermal dependence of the adsorption flux on surface population σ; mobility

This dependence is obtained by plotting $k_A g(\sigma)$ (slope of the straight lines $d\sigma/dt = F(p_0)$) as a function of σ for different constant temperatures (see Fig. 10). By definition, such curves differ from the usual sticking probability versus coverage curves $s(\sigma)$ by the fact that they represent the behaviour of the adsorption flux proper, whatever T and σ.

In reality, they differ from $s(\sigma)$ curves for all temperatures except 0° and 20°C, for which they are rigorously superposable with $s(\sigma)$ curves. This fact probably means that this temperature range is the only range for which no desorption from any of the adsorbed phases is observable.

It can be noted that all the $g(\sigma)$ curves begin with an initial plateau up to an absolute coverage θ of about 20%. For instance, this absolute coverage corresponds to the maximal population for 40°C at $4 \cdot 10^{-8}$ Torr, which means that under these experimental conditions the adsorption flux proper remains constant along the whole adsorption reaction.

For 50° and 60°C, two plateaus are observable, which could be correlated with a phase transition from phase C to a new phase S, leaving some sites C available again for the adsorption of new hydrogen atoms.

According to the model (see preceding paper), $g(\sigma)$ is expected to be of the form $(\sigma_0 - \sigma)^m$, m being the order of the reaction of adsorption as a function of the concentration of one of the reactants, namely the free sites. But this formal dependence holds only if the reactants are independent, which is obviously not the case for adsorption sites. Apart from $m = 0$, which is the best fit for the initial plateaus ($\theta < 20\%$), no possible value ($m > 0$) is found by curve fitting.

A convenient explanation for an initial plateau is that the reaction of adsorption is a *multistep* reaction, involving an intermediate mobile phase (precursor state).

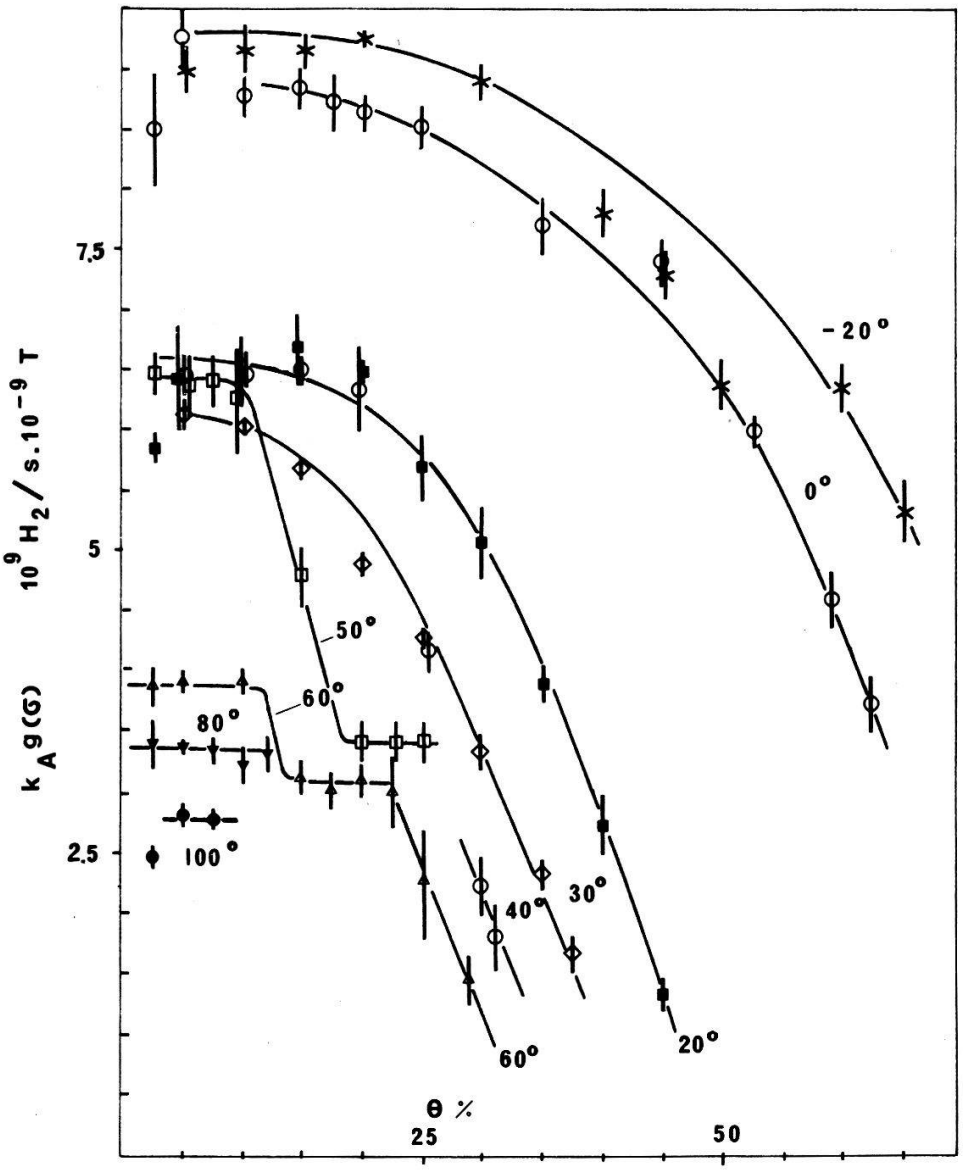

Figure 10
Isothermal dependence of net adsorption flux as a function of surface coverage θ.

5.6. *Isosteric dependence of the adsorption flux on temperature; activation energy E_A for adsorption*

This dependence is obtained by plotting $\ln k_A g(\sigma)$ as a function of $1/T$ for different constant σ. Figure 11 illustrates the dependence for $\sigma = 0$. No activation energy for adsorption E_A is observable, whatever the temperature range. On the contrary, the adsorption flux decreases when temperature increases, especially for high temperature ($T \geqslant 60°C$). The same assumption of a two-step adsorption reaction with an intermediate state, postulated to explain both the dependence of the adsorption flux on pressure (5.4) and on surface population (5.5), can also explain the dependence on temperature.

Figure 11 also illustrates that the correspondence predicted by the kinetic theory of gases between the values of $k_A g(\sigma)$, resulting from our model of interpretation, and the corresponding initial sticking probabilities s_0, as obtained immediately from any of the adsorption curves, is fairly good (volume of incident gas $= 3.638\sqrt{T/M} = 44\ \mathrm{ls}^{-1}$

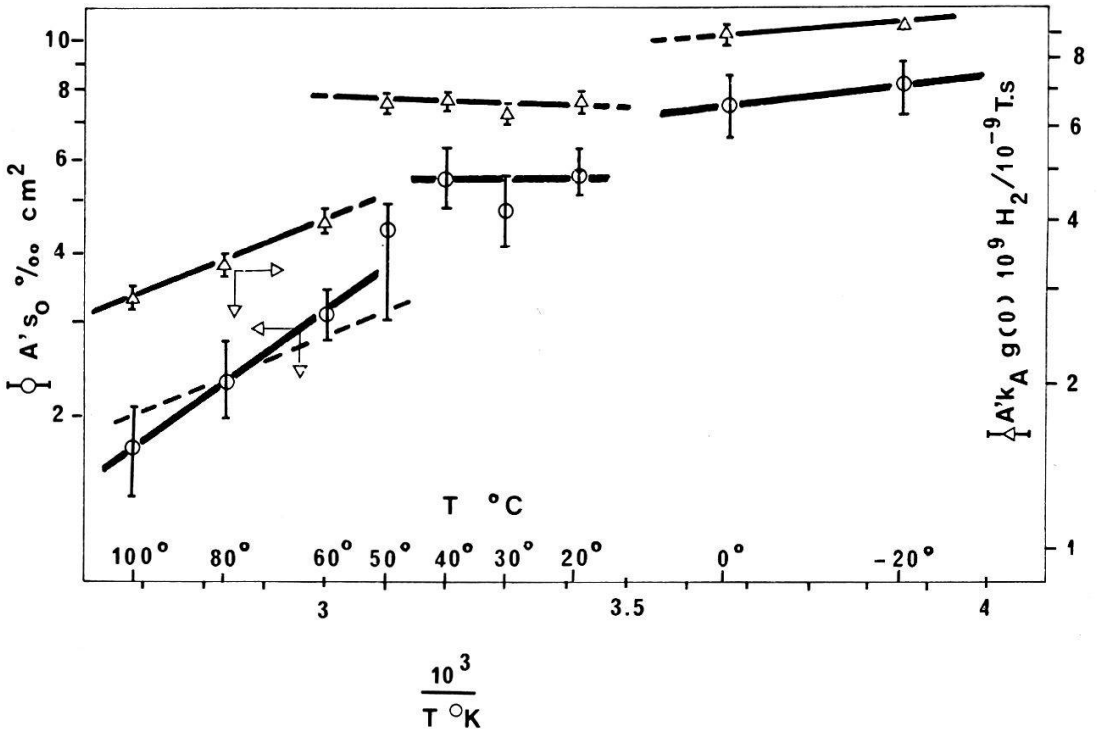

Figure 11
Dependence of the initial sticking probability as a function of temperature. Determination of the activation energy for adsorption E_A.

Table II
Comparative table giving some values of the initial sticking probability s_0 of H_2 on nickel samples, as found in the literature

s_0	Sample	K (°K)	Author(s); reference; date
0.0015	abraded Ni	293	Hoffmann [15]; 1970
0.0036	wire	300	Gasser et al. [16]; 1969
0.005 to 0.01	film	273	Ponec et al. [17]; 1965
0.01	wire		Eisinger [18]; 1958
0.05	ribbon (100) (110)	~300	Lichtman et al. [19]; 1968
>0.1	(110)	293	Germer et al. [20]; 1962
0.17	film	between 78 and 298	Holland [21]; 1965
0.002†	polycrystalline ribbon		Gilbreath and Wilson [22]; 1971
0.003‡			
0.007§			
0.19‖			
0.30	wire (111) and (110)	279	Eley and Norton [23]; 1970
0.34		78	
0.35	film	360	Taylor and Creasy [24]; 1971
0.55		78	
0.35	film	373	Horgan and King [25]; 1971
0.65		78	

† Without treatment.
‡ Oxidation at 1000°K + several oxidation reduction under H_2 at 800°K.
§ As in ‡ + treatment under H_2 at 1100°K.
‖ Freshly deposited film.

cm^{-2} for H_2 at 297°K $= 1.44 \cdot 10^{12}$ H_2 s^{-1} cm^2 at 10^{-9} Torr $= k_A g(0)$ according to the units used for $k_A g(\sigma)$; $A' k_A g(0) = k_A g(0)$ observed $= 1.44 \cdot 10^{12} A' s_0$).

The initial sticking probability s_0 at 77°K is 1 and $s_0 = 0.71 \pm 0.05$ at 300°K. When compared to some data published in the literature (see Table II), these values agree with the most recent values of Horgan and King [25] and Taylor and Creasy [24], and also with those of Eley and Norton found at 279°K, if it is remembered that the number of available sites on a freshly abraded surface is just double that observed on a normal Ni surface. In both cases, s_0 per free site is the same (0.5 at 77°K and 0.35 at room temperature).

5.7. *Isothermal dependence of the desorption flux on surface population σ; order of the desorption reaction*

This dependence is obtained by plotting $\ln k_D h(\sigma)$ (intercept with the origin of the straight line $d\sigma/dt = F(p_0)$) as a function of $\ln \sigma$ for different constant temperatures. According to the definition of $h(\sigma)$ [1], it is expected to be of the form σ^m, with $m =$ order of the desorption reaction. Consequently, the log-plot is expected to be a straight line with slope m.

As illustrated in Figure 12, this is the case for –20°, 0°, 20°, 30° and 40°C with $m = 2$. For 50°C and higher temperature, the very good alignment disappears for low population. Moreover, the desorption fluxes $k_D h(\sigma)$ at 100°C are much too low when compared to the corresponding values at 80°C.

The assumption of a surface phase transition can account for both the apparent change in the order of reaction and the similarity of the thermal desorption fluxes between 80° and 100°C, if we realize that the desorption flux out of a phase depends on the population of *this particular phase*, which can differ from the total surface population, estimated from the loss of gas from the gas phase.

Let us assume the existence of a surface reaction, other than thermal desorption, capable of depopulating the main adsorption phase (C) and to feed another phase (S) from which the desorption flux is negligible. Under such conditions, the population responsible for the measured desorption flux is lower than that appearing on the population scale.

Let σ_G be the amount of gas adsorbed out of the gas phase, σ_S the loss of the desorbing phase, σ_C the actual population of this phase.

$$\sigma_C = \sigma_G - \sigma_S$$

$$k_D h(\sigma_C) = k_D h(\sigma_G - \sigma_S) = k_D(\sigma_G - \sigma_S)^2 = k_D \sigma_G^2 \left(1 - \frac{\sigma_S}{\sigma_G}\right)^2$$

$$\ln k_D h(\sigma_C) = 2 \ln k_D \sigma_G + 2 \ln \left(1 - \frac{\sigma_S}{\sigma_G}\right)$$

Since Figure 12 represents $\ln k_D h(\sigma_C)$ as a function of $\ln \sigma_G$, the plot gives a straight line only in the case where $\sigma_S = 0$, or $\sigma_G \gg \sigma_S$. Where $\sigma_S \neq 0$, $\ln[1 - (\sigma_S/\sigma_G)]$ becomes negative, which tends to decrease the slope. For $\sigma_S/\sigma_G =$ constant, the slope is again 2, but the straight line is shifted downwards.

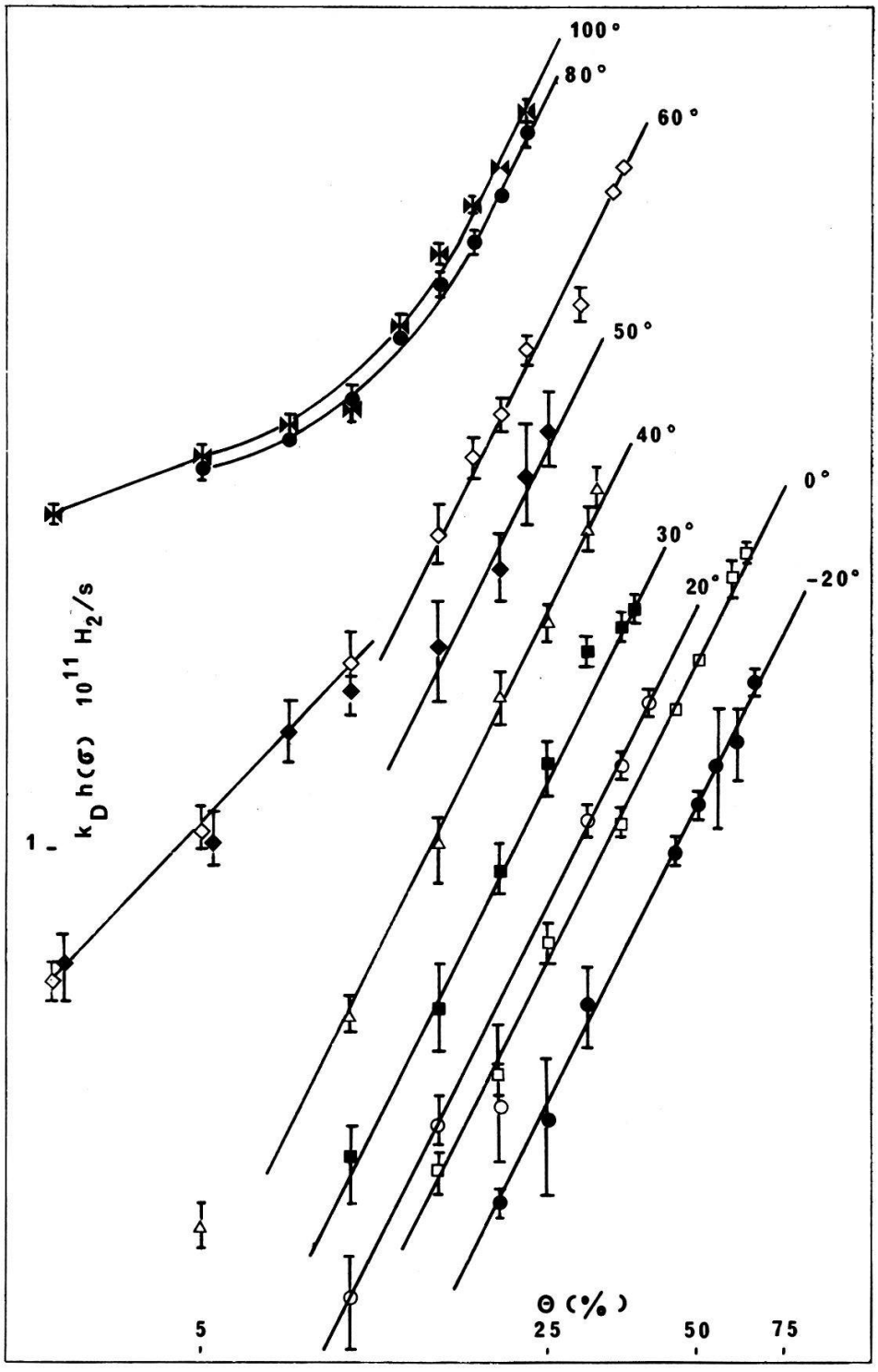

Figure 12
Dependence of the net desorption flux as a function of surface coverage θ. Determination of the order of the reaction of desorption.

It is easy to demonstrate by the same way that, if σ_S represents a supply of phase C other than the adsorption from the gas phase (by diffusion out of the bulk for instance), the trend is to decrease the slope similarly. For σ_S/σ_G = constant, the slope is again 2, but the straight line is shifted upwards.

The conclusion is that the desorption of H_2 adsorbed on Ni is a second-order reaction, whatever the investigated temperature range, the departure from second-

order behaviour for low surface population and the apparent similarity between desorption fluxes at high temperature (80°–100°C) being evidence of a surface phase transition.

5.8. *Isosteric dependence of the desorption flux on temperature; activation energy E_D for desorption; pre-exponential factor k_{D0}*

This dependence is obtained by plotting $\ln k_D h(\sigma)$ as a function of $1/T$ for different constant surface populations. One expects to find straight lines, the slope of which is a measure of the activation energy E_D for desorption $[k_D = k_{D0} \exp(-E_D/RT)]$.

As illustrated in Figure 13, this is the case for temperature higher than 0°C. The slope is slightly dependent on the coverage in the investigated range ($10\% < \theta < 50\%$), decreasing from 14.8 ± 0.5 kcal/mole for $\theta = 10\%$ down to 13.3 ± 0.4 kcal/mole for $\theta = 50\%$ (i.e. 1 H/1 Ni). In an Arrhenius plot, however $[\ln k_D(h(\sigma)/T)$ versus $1/T]$, the slope is independent of the coverage and gives $E_D = 13.5 \pm 0.2$ kcal/mole (see Fig. 9).

There is a discontinuity below 20°C, which shows the existence of a third adsorption phase. The number of experiments in this temperature range is too small for the activation energy of desorption for this low temperature atomic phase to be properly defined. The upper limit estimated from the slope of the graph is 4.7 kcal/mole. This value has no physical meaning because, in this temperature range, the determinations of $k_D h(\sigma)$ at constant overall population are in fact at variable population for each phase, since both phases are populated, and both phases contribute to the overall desorption flux.

Once E_D and $h(\sigma)$ are determined as mentioned above, the desorption rate constant k_D and the pre-exponential factor k_{D0} can be calculated. The unit for k_D is s^{-1}, whatever the order of the reaction, but the numerical value depends on the order of the reaction and of the definition of unit concentration (standard state).

Following Armand and Lapujoulade [26], the standard was chosen to be the monolayer. Under such a condition, $k_{D0} = (1.7 \pm 0.2) \cdot 10^{11}\ s^{-1}$ for $E_D = 14.3$ kcal/mole, whatever T between 20° and 80°C. In contrast to the reaction of adsorption, the pre-exponential factor for the desorption rate is smaller than the value kT/h ($6.1 \cdot 10^{12}\ s^{-1}$ at 20°C) predicted by the absolute reaction rate theory [27]. If the desorption reaction is a one-step reaction, the product $r \cdot \exp(\Delta S/R)$ of the transmission coefficient r times the entropy term (or partition functions ratio), which accounts for the ratio between kT/h and the actual value, is about 0.025.

If r is assumed to be 1, the entropy term (or the partition functions ratio) is 0.025, which means that the ratio between the number of configurations leading to the desorption and the total number of possible configurations of the H atom in the activated state is small.

If $\exp(\Delta S/R)$ is assumed to be 1, $r = 0.025$. This relatively low value could be explained if the H_2^* complex, issued from the combination of two adsorbed H atoms, has a low coupling with the surface and cannot therefore transfer its excess of energy. The probability for the combination of two isolated H atoms into a H_2 molecule in absolute vacuum is extremely low, because the intermediate H_2^* complex has an excess of energy with an extremely short lifetime leading mainly to a redissociation into two H atoms. Theoretical calculations of the transmission coefficient for this particular reaction give values as low as 10^{-12}. When the excess energy of H_2^* can be transferred to a third body, which stabilizes H_2^*, the probability for the combination may come close to 1.

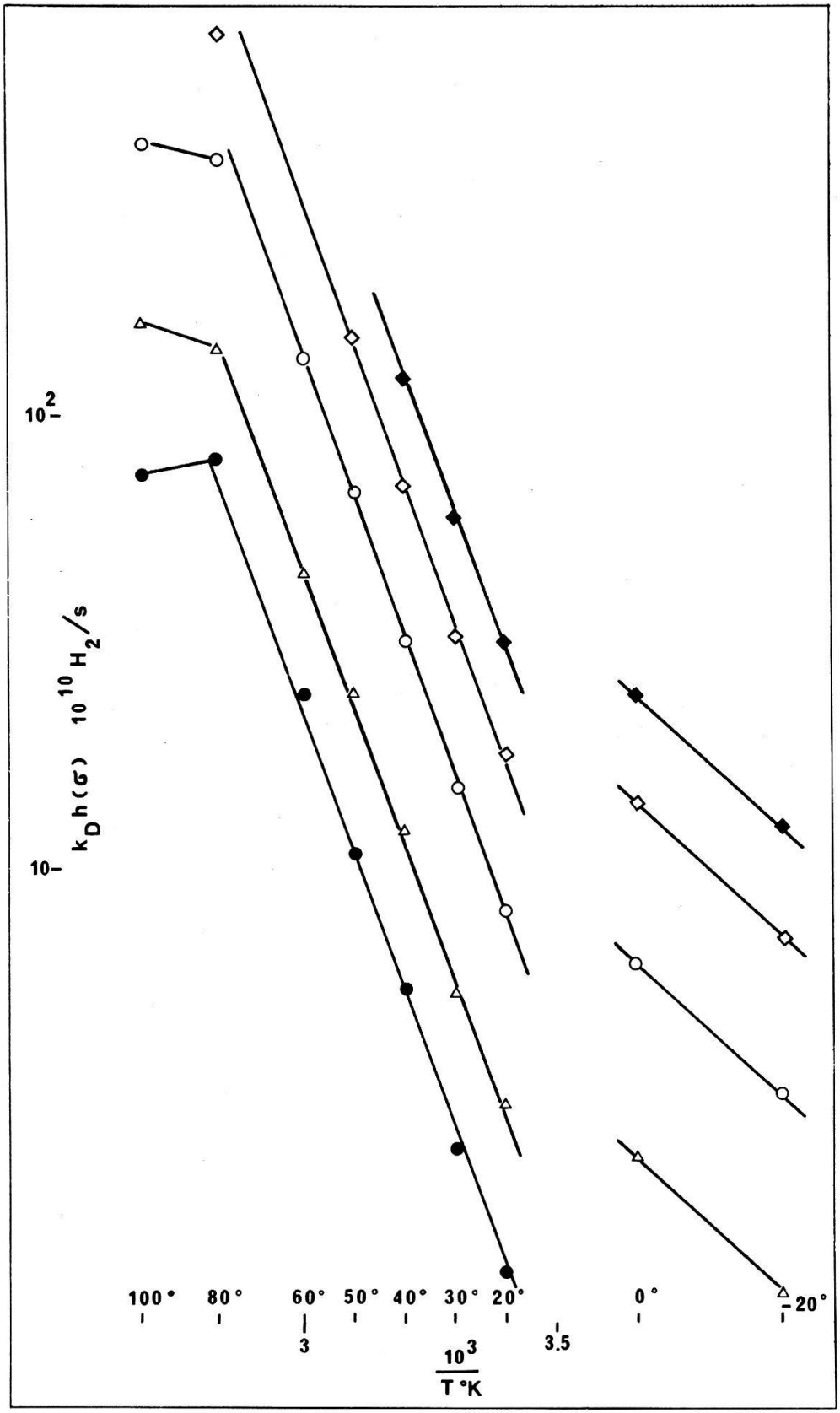

Figure 13
Dependence of the net desorption flux as a function of the reciprocal temperature $1/T$ for different constant surface coverages θ. Determination of the activation energy for desorption E_D. ●: $\theta = 10\%$; △: 15%; ○: 25%; ◇: 37.5%; ◆: 50%.

Let us imagine the desorption reaction as resulting from a similar combination of two adsorbed H atoms giving a H_2^* complex; k_{D0} can then take all values between 10^{-12} and 1, among which is 0.025.

6. Discussion

6.1. Adsorption enthalpy and activation energy for desorption

From the equilibrium measurements, the heat of adsorption is found to be 14.5 ± 0.5 kcal/mole, independently of surface population σ up to a coverage corresponding to about 1 H/1 Ni ($\theta = 50\%$).

Both initial value and constancy as a function of θ are confirmed by the independent kinetic measurements of the activation energy for desorption. When compared with the data published in the literature (see Table III), it can be noticed that these data agree with recent data from Wedler and Bröcker [45], Martin et al. [44] and Ertl and Küppers [43].

Table III
Comparative table giving some values of the binding energy of H_2 on Ni at zero coverage, as found in the literature

ΔE; ΔH [kcal/mole]	Sample	Comments	Author(s); date
56 (279°K) 50 (78°K)	wire	Heat of adsorption; q decreases down to 0 when θ increases	Eley and Norton [23]; 1970
46 ± 4	tip	FEM at 4.2°K; E_D	Wortmann et al. [28]; 1957
43 ± 2	film	linear decrease of ΔH with coverage	Klemperer and Stone [29]; 1957
34	Ni-Kieselguhr (52.8% Ni)	magnetic measurements; linear decrease of the differential heat of adsorption down to 0 for $\theta = 1$	Lee et al. [30]; 1957
33 (450°K)	(111)	linear decrease with θ down to 10 kcal/mole for θ_m	Lapujoulade [31]; 1971
32	film	isosteric heat at 300°K; sharp drop with θ down to ~24 kcal/mole; after much slower decrease	Rideal and Sweet [32]; 1960
31 ± 2	film	ΔH; slow decrease down to 26 kcal/mole up to $\theta = 0.5$; after much steeper (15 kcal/mole for $\theta = 1$)	Beeck [33]; 1950
~30	Ni–silica	adsorption heat; variation of magnetic susceptibility; decrease with θ	Selwood [34], 1967
29 ± 1	film	calorimetry; decrease analogous to Beeck	Wahba and Kemball [35]; 1953
27	powder	ΔH; linear decrease with θ	Roberts and Sykes [36]; 1958
26	powder	ΔH	Kwan [37]; 1949
26 ± 1	silica supported Ni	isosteric heat	Stevenson [38]; 1955
25.5 ± 1	silica supported Ni	isosteric heat	G. C. A. Schuit [39]; 1957

Table III—*continued*

ΔE; ΔH [kcal/mole]	Sample	Comments	Author(s); date
25	film	calorimetry	Brennan and Hayes [40]; 1964
24	powder	ΔH; linear decrease with θ	Shield and Russel [41]; 1960
23	film	isosteric heat; $\gamma = 10^{13}\ s^{-1}$; slow decrease down to 18 kcal/mole	Taylor and Creasey [24]; 1972
23.4	film	activation energy of TD; this value is 12 kcal/mole for dirty films	Gilbreath and Wilson [22]; 1971
22	(111)	activation energy of TD; constant up to $\sigma = 6 \cdot 10^{12}\ H_2/cm^2$	Lapujoulade, 1972, private communication
21	powder	ΔH; linear decrease with θ	Eucken [42]; 1949
19.5 ± 10%	(110)	isosteric heat; independent of θ up to $\theta = 0.5$	Ertl and Küppers [43]; 1971
19	Ni/silica; monocristal	isosteric heat; q depends or not on θ according to Ni samples	Martin et al. [44]; 1972
18 ± 0.7	film	calorimetry; heat of desorption	Bröcker and Wedler [45]; 1966
17	film	E_D	Gasser et al. [16]; 1969
15–16	(110)	E_D; depends on θ	Lapujoulade, 1972, private communication
15.6	film	calorimetry; heat of adsorption; independent of θ up to 0.85 H/Ni	Bröcker and Wedler [45]; 1966
11.5	film	slightly oxidized Ni film; molecular beam	Dewing and Robertson [46]; 1957
10.8	polycrystalline disc		Lapujoulade [47]; 1967
6.5	film		Suhrmann et al. [48]; 1959

The value of ΔH agrees also with the estimation by means of the Pauling's expression valid for covalent bonding:

$$-\Delta H = 2D_{MH} - D_{HH}$$

with

$$D_{MH} = \tfrac{1}{2}(D_{MM} + D_{HH}) + 23.06\,(\kappa_M - \kappa_H)^2$$

$D_{HH} = 103.2$ kcal/mole = dissociation energy for H_2

κ = electro-negativity

The results obtained from this expression differ somewhat according to the assumptions adopted for κ, but Bond [14] mentions several values close to 17 kcal/mole in disagreement with the experimental values (29 → 32 kcal/mole) to which they were compared at that time.

Since ΔH (and E_D) are independent of the coverage θ, this is consistent with the assumption that an abraded surface is initially homogeneous, that no heterogeneity is induced in the course of adsorption, and that the lateral H—H interactions are weak.

Some possible explanations are:

— heat does not depend on crystallographic orientation; the heterogeneity, when observed, is due essentially to chemical impurities, not to physical defects;
— the notion of crystal plane has no meaning on an amorphous abraded surface, built up mainly by similar surface defects;
— H_2 does not adsorb 'on' but 'below' the outermost Ni atoms layer, where surface defects have much less influence.

6.2. *Activity of freshly abraded surfaces*

It is shown that the H_2 coverage at saturation is 2 H/1 Ni, which is double the value reported for ultraclean Ni surfaces. This fact explains why the initial sticking probability s_0 at room temperature (0.7) is also double the highest value (0.35) published in the literature.

$s_0(O_2/Ni) = 1$ from 77° up to 520°K with a surface saturation of 2 O/1 Ni [11]; $s_0(CO) = 1$ at 77° and 300°K with a surface saturation of 1 CO/1 Ni.

It is clearly established that the chemical reactivity of a fresh surface is quite high. The question open for discussion is whether this is due only to the extreme cleanliness or to excited states characteristic of fresh surfaces only. Contradictory statements are found in the literature regarding this subject [49–54].

6.3. *Application of the treatment model to data resulting from thermal desorption at constant temperature*

The model adopted to calculate the parameters of the gas/solid interaction from adsorption data is based only on the ability of measuring variations of surface population $d\sigma/dt$ at constant temperature, without specifying the sign of $d\sigma/dt$. When positive, $d\sigma/dt$ means an increase of surface population by isothermal adsorption, with adsorption flux greater than the desorption flux. When negative, $d\sigma/dt$ means a decrease of surface population by isothermal desorption, with readsorption flux lower than the desorption flux. The last experimental situation can be achieved if a step of temperature is imposed on the sample.

In order to check the self-consistency of the model of treatment, a set of experiments was conducted in the following conditions:

— passivation of the inner surface of the Ni tube, by means of a slight oxidation (3 mn at 800°C below 10^{-6} Torr O_2), which reduces the sticking probability and the surface population of at least two orders of magnitude [22];
— abrasion of a large zone (50 to 100 × G_2) under p_{0i} at 20°C;
— temperature step from 20°C to 30°C with registration of the thermal desorption curve;
— temperature step from 30°C to 40°C with registration of the thermal desorption curve;
— temperature drop from 40°C to 20°C with registration of the adsorption curve as a check for correspondence between the sum of desorbed H_2 amounts and uptake during the cycle.

The same cycle ($20° \rightarrow 30°$, $30° \rightarrow 40°$, $40° \rightarrow 20°$) was repeated under p_{0j} ($j \neq i$), for six different p_{0j}.

The dependence between $d\sigma/dt$ and p_{0j} is found to be linear. The resulting straight lines of the $d\sigma/dt = F(p_{0j})$ plot line up reasonably well with the corresponding straight lines obtained by adsorption measurements. The agreement could be perfect if the progressive passivation of the abraded Ni surface in course of time (indicated by the check of amounts desorbed/readsorbed for each cycle and probably due to diffusion of impurities) were taken into account.

In conclusion, it has been proved by thermal desorption experiments at constant temperature that the model of treatment is consistent and that thermal desorption is an unsuitable technique for reliable measurements, due to inevitable pollution (at least long term) by the gas phase and/or by impurity diffusion from the bulk (apart from the possibility of thermally induced surface phase transition preceding the desorption proper).

6.4. Determination of the order of the desorption reaction from thermal desorption curves at constant temperature

Since extreme care had been taken to record high-quality desorption curves under constant temperature, it was decided to use some of the best curves to determine the order of the reaction of thermal desorption by the usual ways and compare with the result issued from application of the model.

As the curves are found to have an exponential decay, the order of reaction is one, when no particular variation of E_D with θ is assumed and no readsorption accounted for, which seems justified, as is frequently the case.

In fact the order is really 2, but the readsorption is not negligible and follows such a kinetics that the desorption curve (like the adsorption curve) is made up of two exponential functions [5].

This example illustrates the fragility of some tests, based on single data, when compared to the reliability of the test by the $h(\sigma)$ plot, based on a set of data, and without assumption regarding a possible negligible counter flux.

7. Summary and Conclusions

The picture of the H_2 interaction with a freshly abraded Ni surface resulting from the application of the model of treatment to abrasion-induced adsorption measurements is the following.

There are four adsorption phases:

— a molecular physisorbed phase significantly populated only at low temperature;
— a mobile atomic phase P, precursor of phase C, significantly populated only below 20°C, with a maximum population corresponding to 1 H/1 Ni;
— an atomic chemisorbed phase C, the major phase responsible for what is observed above 20°, with a maximum population corresponding to 1 H/1 Ni;
— an atomic phase S, probably representative of 'bulk' hydrogen.

The overall adsorption reaction is not activated; it is a two-step reaction involving a mobile atomic precursor state (phase P).

The adsorption heat corresponding to phase C is 14.5 kcal/mole and independent of the population of this phase. The adsorption heat for phase P is lower and probably decreases with population.

The surface reaction from C to S and vice versa is activated.

The desorption from phase C is a one-step second-order reaction, the activation energy of which is about 14 kcal/mole.

The desorption from phase P is a second-order reaction, the activation energy of which is lower than 4 kcal/mole.

These results show that abrasion can constitute a powerful, ultraclean and reliable technique for investigation of H_2/Ni interaction. This statement is probably true whatever the gas and the abraded surface.

Acknowledgments

The author wishes to express his gratitude to the Directors of the Battelle Geneva Research Centre, which has supported this research, to Dr. L. A. Petermann for numerous and fruitful discussions, and to Professor J. P. Borel, of the Swiss Institute of Technology, Lausanne, for having supervised this thesis work.

REFERENCES

[1] J. F. ANTONINI, preceding paper.
[2] J. F. ANTONINI, Supp. Nuovo Cim. *5* (2), 354 (1967).
[3] J. F. ANTONINI. G. HOCHSTRASSER and P. ACLOQUE, Verre & Refrac. *23* (2), 169 (1969).
[4] J. F. ANTONINI, Proc. IVth Intern. Vacuum Cong. p. 179, Manchester (1968).
[5] J. F. ANTONINI, Thesis, Federal Institute of Technology, Lausanne, Switzerland (1973).
[6] U. A. MCRAE, Surf. Sci. *1*, 319 (1964).
[7] A. M. HORGAN and D. A. KING, *Structure and Chemistry of Solid Surfaces*, edited by SOMORJAI (J. Wiley, New York, 1969).
[8] L. H. GERMER, J. W. MAY and R. J. SZOSLAK, Surf. Sci. *8*, 430 (1967).
[9] J. EISINGER, J. Chem. Phys. *30*, 412 (1959).
[10] A. KLOPFER, Ber. Bunsen Ges. *75* (10), 1071 (1971).
[11] J. F. ANTONINI, to be published.
[12] P. M. GUNDRY and F. C. TOMPKINS, Trans. Farad. Soc. *52*, 1609 (1956).
[13] P. M. GUNDRY and F. C. TOMPKINS, Trans. Farad. Soc. *53*, 218 (1957).
[14] G. C. BOND, *Catalysis by Metals* (Academic Press, London and New York 1962).
[15] H. HOFFMANN, Z. für Phys. Chem. *245*, 37 (1970).
[16] R. P. H. GASSER, K. ROBERTS and A. J. STEVENS, Trans. Farad. Soc. *65*, 3105 (1969).
[17] V. PONEC and S. CERNY, Rozpravy Ceskoslov. Akad.; Ved. Radamet prirodnich Ved *75*, 32 (1965).
[18] J. EISINGER, J. Chem. Phys. *29*, 1154 (1958).
[19] D. LICHTMAN, F. N. SIMON and T. R. KIRST, Surf. Sci. *9* (2), 325 (1968).
[20] L. H. GERMER and A. U. MCRAE, J. Chem. Phys. *37*, 1383 (1962).
[21] L. HOLLAND, Brit. J. Appl. Phys. *16*, 1053 (1965).
[22] W. P. GILBREATH and D. E. WILSON, J. Vac. Sci. & Techn. *8* (1), 45 (1971).
[23] D. D. ELEY and P. R. NORTON, Proc. Roy. Soc. A *314*, 319 (1970).
[24] N. TAYLOR and R. CREASY, *Adsorption–Desorption Phenomena*, edited by F. RICCA (Academic Press, London 1972), p. 297.
[25] A. M. HORGAN and D. A. KING, *Adsorption–Desorption Phenomena*, edited by F. RICCA (Academic Press, London 1972), p. 329.
[26] G. ARMAND and J. LAPUJOULADE, Surf. Sci. *6*, 345 (1967).
[27] S. GLASSTONE, K. J. LEIDLER and H. EYRING, *The Theory of Rate Processes* (McGraw-Hill, New York, 1941).
[28] R. WORTMAN, R. GOMER and R. LUNDY, J. Chem. Phys. *27*, 1099 (1957)
[29] D. F. KLEMPERER and E. S. STONES, Proc. Roy. Soc. A *243*, 375 (1957).
[30] E. L. LEE, J. A. SABATKA and P. W. SELWOOD, J. Amer. Chem. Soc. *79*, 5391 (1957).
[31] J. LAPUJOULADE, J. de Chim. Phys. *68* (1), 73 (1971).
[32] E. K. RIDEAL and F. SWEET, Proc. Roy. Soc. A *257*, 291 (1960).
[33] O. BEECK, Disc. Farad. Soc. *8*, 118 (1950).

[34] P. W. Selwood, *The magnetic properties of solid–gas interface*, in *The Solid–Gas Interface*, edited by E. Alison Flood (Marcel Dekker, New York 1967).
[35] M. Wahba and C. Kemball, Trans. Farad. Soc. *49*, 1351 (1953).
[36] M. W. Roberts and K. W. Sykes, Trans. Farad. Soc. *54*, 548 (1958).
[37] T. Kwan, J. Res. Inst. Catal. Hokkaido Univ. *1*, 81 (1949).
[38] O. P. Stevenson, J. Chem. Phys. *23*, 203 (1955).
[39] G. C. A. Schuit, *Chemisorption* (Butterworth, London 1957).
[40] D. Brennan and F. H. Hayes, Trans. Farad. Soc. *60*, 589 (1964).
[41] L. S. Shield and W. W. Russel, J. Phys. Chem. *64*, 1592 (1960).
[42] A. Eucken, Z. Elektrochem. *53*, 285 (1949).
[43] G. Ertl and D. Küppers, Ber. Bunsen Ges. *75* (10), 1017 (1971).
[44] G. A. Martin, G. Dalmai-Imelik and B. Imelik, *Adsorption–Desorption Phenomena*, edited by F. Ricca (Academic Press, London 1972).
[45] F. J. Bröcker and G. Wedler, Disc. Farad. Soc. *41*, 87 (1966).
[46] J. Dewing and A. J. B. Robertson, Proc. Roy. Soc. A *240*, 423 (1957).
[47] J. Lapujoulade, Suppl. Nuovo Cimento *5*, II, 433 (1967).
[48] R. Suhrmann, Y. Mizushima, A. Hermann and G. Wedler, Z. Phys. Chem. NF (Frankfurt) *20*, 332 (1959).
[49] W. M. Sachtler, C. R. Kiliszek and B. E. Nieuwenhuys, Thin Solid Films *2*, 43 (1968).
[50] D. R. Palmer, S. R. Morrisson and C. E. Dauenbaugh, Phys. Rev. Letters *6*, 170 (1961).
[51] M. Green, J. Phys. Chem. Solids *14*, 77 (1960).
[52] A. J. Rosenberg, P. H. Robinson and H. C. Gatos, J. Appl. Phys. *29*, 771 (1958).
[53] J. R. Anderson and R. J. MacDonald, J. Catal. *13*, 345 (1969).
[54] T. Takeuchi, Y. Nakashima, Y. Tezuka and D. Miyatani, Naturwissenschaften *58* (1), 52 (1971).